Membrane lipids and their degradation compounds control GM2 catabolism at intralysosomal luminal vesicles

Susi Anheuser, Bernadette Breiden, and Konrad Sandhoff

Membrane Biology and Lipid Biochemistry Unit, Life and Medical Sciences Institute, University of Bonn, Bonn, Germany

ORCID IDs: 0000-0003-1029-3137 (S.A.); 0000-0002-4838-4109 (B.B.); 0000-0003-2452-8654 (K.S.)

Abstract The catabolism of ganglioside GM2 is dependent on three gene products. Mutations in any of these genes result in a different type of GM2 gangliosidosis (Tay-Sachs disease, Sandhoff disease, and the B1 and AB variants of GM2 gangliosidosis), with GM2 as the major lysosomal storage compound. GM2 is also a secondary storage compound in lysosomal storage diseases such as Niemann-Pick disease types A–C, with primary storage of SM in type A and cholesterol in types B and C, respectively. The reconstitution of GM2 catabolism at liposomal surfaces carrying GM2 revealed that incorporating lipids into the GM2-carrying membrane such as cholesterol, SM, sphingosine, and sphinganine inhibits GM2 hydrolysis by β-hexosaminidase A assisted by GM2 activator protein, while anionic lipids, ceramide, fatty acids, lysophosphatidylcholine, and diacylglycerol stimulate GM2 catabolism. In contrast, the hydrolysis of the synthetic, water-soluble substrate 4-methylumbelliferyl-6-sulfo-2-acetamido-2-deoxy-β-D-glucopyranoside was neither significantly affected by membrane lipids such as ceramide or SM nor stimulated by anionic lipids such as bis(monoacylglycero)phosphate added as liposomes, detergent micelles, or lipid aggregates. Moreover, hydrolysis-inhibiting lipids also had an inhibiting effect on the solubilization and mobilization of membrane-bound lipids by the GM2 activator protein, while the stimulating lipids enhanced lipid mobilization.—Anheuser, S., B. Breiden, and K. Sandhoff. **Membrane lipids and their degradation compounds control GM2 catabolism at intralysosomal luminal vesicles.** *J. Lipid Res.* 2019. 60: 1099–1111.

Supplementary key words lipid transfer protein • sphingolipids • gangliosides • cholesterol • sphingomyelin • bis(monoacylglycero)phosphate • sphingosine • solubilization • enzymology

vesicles (ILVs) are the platform for the catabolism of membrane lipids (1). Their lipid composition varies from the limiting endosomal and lysosomal perimeter membranes by a much lower cholesterol (Chol) content, an enhanced occurrence of bis(monoacylglycero)phosphate (BMP) (2–4), and the absence of a glycocalix. A disturbance of the physiological lipid composition in the lysosomal system may well contribute to the molecular and clinical pathology of a multitude of lysosomal storage disorders (5, 6).

To enable a physiological turnover of membrane lipids, they have to reach the ILVs of the endolysosomal system, e.g., by endocytotic membrane flow. Along the endocytotic pathway the lipid composition of the intraendolysosomal vesicles to the ILVs changes radically. Plasma membrane stabilizing lipids are sorted out; e.g., Chol is secreted by Niemann-Pick protein types 1 and 2 (7–9). In addition, the anionic BMP accumulates as an intermediate of phosphatidylglycerol catabolism (10), whereas a multiplicity of membrane lipids is depleted, e.g., SM by degradation (11, 12). Proper catabolism of sphingolipids with short oligosaccharide head groups requires special lipid binding and transfer proteins, so-called sphingolipid activator proteins, that mediate the interaction of the membrane-bound lipid substrate and the water-soluble enzyme (13–16). They consist of the saposins A–D and the GM2 activator protein (GM2AP).

It is known that (glyco)sphingolipid hydrolysis is enhanced by BMP (17–25), an anionic lipid of the ILVs, which is of functional significance and acts as a stimulating

Amphiphilic lipids and proteins are ubiquitous building blocks of biological membranes that preserve specific patterns in subcellular membranes. Intralysosomal luminal

lipid modifier (23). It places negative surface charge to the luminal vesicles (18, 22, 23), even at the low pH range in the lysosome (pH 4–5) (26, 27). The GM2AP possesses an isoelectric point around pH 4.8 (15), caused by the stacked occurrence of lysine residues, that results in positively charged surface domains at low lysosomal pH values and makes an allowance to the interaction with the ILVs covered by a negative zeta potential that becomes more negative by the anionic membrane-bound BMP and other anionic lipids (22).

The GM2AP, which is known to be a quite promiscuous lipid binding protein (28, 29), forms a stoichiometric complex with membrane-bound ganglioside GM2, which is recognized by β-hexosaminidase A (Hex A), forming a soluble Michaelis-Menten complex (14, 30). Until now, it has not exactly been known whether the catabolism of GM2 takes place at the surface of the ILVs, in solution, or at both locations simultaneously. Mutations that affect the function of Hex A or GM2AP can inhibit the crucial catabolic pathway, resulting in lysosomal storage diseases such as Tay-Sachs disease, Sandhoff disease, and the AB or B1 variants of GM2 gangliosidosis (31). Furthermore GM2 accumulates as a secondary storage compound in different lysosomal storage disorders, e.g., in Niemann-Pick disease (32, 33) and in different mucopolysaccharidoses (34).

SM or Chol are the primary storage compounds in Niemann-Pick disease types A and B and C, respectively. The hydrolysis of GM2 is inhibited by both lipids (23). We analyzed the influence of other membrane lipids and their degradation intermediates occurring in the lysosomal compartment, ceramide (Cer), fatty acids, lysophosphatidylcholine (lyso-PC), diacylglycerol (DAG), sphingosine (So), and sphinganine (Sa). All tested lipids influenced the catabolism of membrane-bound GM2 by Hex A and were assisted by GM2AP substantially, while the turnover of the synthetic, water soluble substrate 4-methylumbelliferyl-6-sulfo-2-acetamido-2-deoxy-β-D-glycopyranoside (MUGS) by Hex A was not affected by membrane lipids.

MATERIALS AND METHODS

Materials

1,2-Dioleoyl-*sn*-glycerol-3-phosphocholine (DOPC), So, and C18:1-BMP were purchased from Avanti Polar Lipids (Alabaster, AL). GM2 and D-*erythro*-stearoyl-Cer were available in our laboratory. Chol, 1,2-dipalmitoylglycerol (DAG), Sa, lysopalmitoyl-PC, stearic acid, 4-methylumbelliferone (MUF), and MUGS were purchased from Sigma-Aldrich (Taufkirchen, Germany). Stearoyl-SM was from Matreya (State College, PA). All other chemicals were obtained from Merck (Darmstadt, Germany) and Sigma-Aldrich and were of analytical grade.

Synthesis of [^{14}C]GM2

[^{14}C]GM2 was synthesized from its corresponding lysolipid following published procedures (35).

Protein preparation

Glycosylated recombinant GM2AP (g-rGM2AP) and g-rGM2AP with hexahistidine-tag (His$_6$) was prepared as described previously

(23). Hex A was purified from human placenta to apparent homogeneity as described previously (36).

Preparation of liposomes

Large unilamellar vesicles were prepared as previously described (23, 37). Liposomes without BMP contained 5 mol% Chol, 2 mol% assay-specific lipids as [^{14}C]GM2, the lipid of interest (0–40 mol%), and DOPC as a host lipid in 20 mM sodium citrate buffer, pH 4.2. BMP containing liposomes and carrying an additional negative net charge contained 20 mol% BMP. The amount of DOPC was adjusted to the varied lipid composition. The lipid concentration was 50 mM.

Hex A activity assay with soluble substrate MUGS

In this assay, the turnover of MUGS to MUF was measured. Hex A (2 mU) and MUGS (0.25 mM) were incubated in 20 mM sodium citrate, pH 4.2 (final volume: 80 µl), at 37°C for 30 min. After that the assay was stopped with 400 µl stop solution (0.2 M Na$_2$CO$_3$ + 0.2 M glycine, pH 9.8). Fluorescence of the formed MUF was measured with a spectrofluorophotometer (RF-5000; Shimadzu, Düsseldorf, Germany). Fluorescence was measured using an excitation wavelength of 365 nm and an emission wavelength of 440 nm.

In addition to this basic assay, liposomes, Triton-X 100 micelles, or lipid aggregates were added. The lipid composition of all three formulations was 5 mol% Chol, 20 mol% BMP, and 0–40 mol% Cer or SM made up to 100 mol% by DOPC, and the lipid concentration was 50 mM.

The liposomes were prepared as described above. For forming Triton-X 100 micelles, the appropriate amounts of lipids from stock solutions were mixed and dried under a stream of nitrogen. The lipid mixture was then dispersed in 1 ml of 20 mM sodium citrate buffer, pH 4.2, containing 625 µg Triton-X 100. The dispersion was vortexed and sonified in a sonifier bath for 15 min. To build lipid aggregates, the dried lipid mixture was dispersed in 1 ml of 20 mM sodium citrate buffer, pH 4.2. The dispersion was vortexed and sonified for 3 × 3 min (Brandson Sonifier 250; Branson Ultrasonics Corporation, Danbury, CT).

In the case of g-rGM2AP, the added amount was 0.06 pmol. The amount of generated MUF was determined by a straight calibration line of 0, 1, 2, 4, 6, 8, and 10 mol MUF in a volume of 80 µl mixed with 400 µl stop solution.

Liposomal activity assay with GM2AP and Hex A

Vesicles were prepared as described above. The lipid concentration of the vesicles containing 2 mol% [^{14}C]GM2 was 0.5 mM. The assay was done following the published procedure (23).

The 40 µl liposome dispersion was mixed with 2 mU Hex A and *a*) for BMP containing vesicles with 0.06 pmol g-rGM2AP or g-rGMAP-His$_6$, *b*) for vesicles free of BMP with 0.3 pmol g-rGM2AP or g-rGMAP-His$_6$, and then all mixtures were made up to 80 µl with 20 mM sodium citrate buffer, pH 4.2. Different amounts of GM2AP were chosen because the GM2 turnover at membranes free of BMP is quite small (23). The samples were incubated at 37°C for 30 min. The assay was then put on ice and stopped by adding 20 µl chloroform-methanol (1:1; v:v).

The generated [^{14}C]GM3 from [^{14}C]GM2 was quantified by thin-layer chromatography. Therefore, the preparations were dried under a stream of nitrogen, redissolved with 20 µl chloroform-methanol (1:1; v/v), vortexed, and sonified for 15 min. The solution of lipids was applied to a high-performance thin-layer chromatography plate (Merck). Lipids were separated in chloroform-methanol-0.22% CaCl$_2$ (55:45:10; v/v/v).

Radioactive bands were visualized with Typhoon Fla 7000 (GE Healthcare, Buckinghamshire, UK), and the quantification was performed with the image-analysis software Image Quant TL (GE Healthcare).

Lipid mobilization assay by SPR spectroscopy

The lipid mobilization assay was done following the published procedure (23). Surface plasmon resonance (SPR) spectroscopy, a biomolecular interaction analysis, was carried out at 25°C with a Bialite instrument (GE Healthcare).

In the lipid mobilization assay, negatively charged liposomes with 5 mol% Chol, 20 mol% BMP, and 10 mol% GM2 in 20 mM sodium citrate buffer, pH 4.2, were used (unless stated otherwise). Sensor chips providing an immobilized surface with lipophilic anchors attached to a dextran matrix (Pioneer HPA chip) were obtained from Biacore (Uppsala, Sweden). Vesicles (100 µl; 0.5 mM total lipid concentration) in 20 mM sodium citrate buffer, pH 4.2, were injected into the system at a flow rate of 5 ml/min. This resulted in a shift of approximately 2,000 resonance units (RUs), which corresponds to a lipid monolayer (see manual of Pioneer HPA chip). The lipid layer-loaded chip was set as the baseline (RU = 0) and corresponds to 100% of loaded lipid material.

GM2AP (0.2 mM) in running buffer (20 mM sodium citrate buffer, pH 4.2) was injected into the flow cells at a rate of 20 ml/min for 3 min, followed by buffer alone. The RUs above the baseline represent material bound to the lipid layer (e.g., GM2AP) during the experiment, whereas negative RUs below the baseline represent material loss, which not only includes GM2AP added during the experiment but also lipid material mobilized and released from the lipid layer. However, it remains unclear for all data above the baseline (RU = 0) if the loss was due to the removal of lipids or to a removal of both, a mixture of proteins and lipids. Only if the RU value drops below the baseline can we be certain that lipids from the lipid layer have been removed. The release and mobilization of liposomal lipids have been analyzed previously by using radiolabeled membrane lipids (38).

All data presented are the means of at least triplicates.

RESULTS

Whereas soluble macromolecules can be degraded directly by soluble hydrolases, special mechanisms are necessary for the turnover of membrane-bound (glyco)sphingolipids. The lipid binding and transfer protein GM2AP is known to play an essential role in the catabolism of GM2 by Hex A at the ILVs (15). As has been shown previously, the catabolism of GM2 by the water-soluble Hex A occurs in cooperation with GM2AP and is strongly modified by the lipid composition of the GM2-carrying membranes (17, 23, 39). To investigate this coherence more precisely we reconstituted GM2 catabolism at ILVs of the lysosomal compartment in a liposomal system. We then used a lipid mobilization assay to analyze the g-rGM2AP-mediated solubilization of membrane lipids and their degradation products occurring in the lysosomes, such as SM, Chol, DAG, Cer, lyso-PC, free fatty acids, So, and Sa. For comparison, we also analyzed the influence of membrane lipids on the turnover of the synthetic, water-soluble substrate MUGS by Hex A.

The cleavage of soluble MUGS is almost independent of the presence of GM2AP and membrane lipids

The soluble, synthetic substrate MUGS is usually used to assay Hex A activity in research for lysosomal storage disorders (40, 41). It is known that Hex A shows a broad pH profile (3.0–7.6) against soluble, synthetic substrates (42), but an extremely sharp one (pH 3.5–4.6) for the hydrolysis of membrane-bound GM2 in the presence of its cofactor GM2AP (17, 23, 39, 43).

As a control for the strong dependence of GM2 hydrolysis by Hex A in presence of GM2AP on the lipids of the GM2-carrying membranes, such as BMP, Cer, and SM (17, 23), we assayed the influence of membrane lipids on the cleavage of MUGS by Hex A. The MUGS turnover by Hex A was analyzed in the absence and presence of membrane lipids, liposomes, Triton-X 100 micelles, lipid aggregates, and/or g-rGM2AP. Liposomes were used to mimic ILVs, and Triton-X micelles were chosen because Hex A can cleave GM2 bound to detergent micelles (44–47). Lipid aggregates were free of detergent to suspend severe side effects eventually caused by the use of detergent in Triton-X 100 micelles.

The cleavage of MUGS is almost completely independent of GM2AP, the presence of membrane liposomes (**Fig. 1A**), lipid aggregates, or Triton-X 100 micelles (data not shown), while the hydrolysis of membrane-bound liposomal GM2 strongly depends on all of these factors (Fig. 1B).

A physiologically relevant hydrolysis of membrane-bound [^{14}C]GM2 by Hex A was only detectable in the presence of both GM2AP and anionic lipids such as BMP (Fig. 1B, left). The addition of 40 mol% Cer to BMP containing liposomes resulted in a 4-fold stimulation of GM2 catabolism by Hex A in the presence of GM2AP, while the addition of 40 mol% SM to BMP containing liposomes reduced GM2 hydrolysis to 40% (Fig. 1B, right). The GM2AP-independent turnover of the synthetic, soluble substrate by Hex A was independent of the addition of liposomes in every composition (Fig. 1A) and Triton-X 100 micelles or lipid aggregates in similar compositions (data not shown).

Storage compounds of Niemann-Pick diseases, SM, and Chol inhibit GM2 turnover and lipid mobilization

SM is degraded by acid sphingomyelinase to Cer in the late endosomal compartment but accumulates in acid sphingomyelinase-deficient Niemann-Pick disease types A and B. It is known that in Niemann-Pick disease types A and B the storage of SM provokes the secondary accumulation of Chol. However, the storage of Chol in Niemann-Pick disease type C triggers the secondary accumulation of SM (48, 49). We showed previously that both lipids are of great significance for the catabolism of liposomal-bound GM2 (23). Using liposomal reconstitution experiments that consisted of liposomes carrying [^{14}C]GM2, which cannot leave the membrane spontaneously because of its hydrophobic Cer tail (containing two long hydrophobic chains), we analyzed those coherences more precisely (**Fig. 2**, **Fig. 3**). On the other hand, we used lipid mobilization assays to analyze the lipid solubilization properties of GM2AP (**Fig. 4**). The RUs
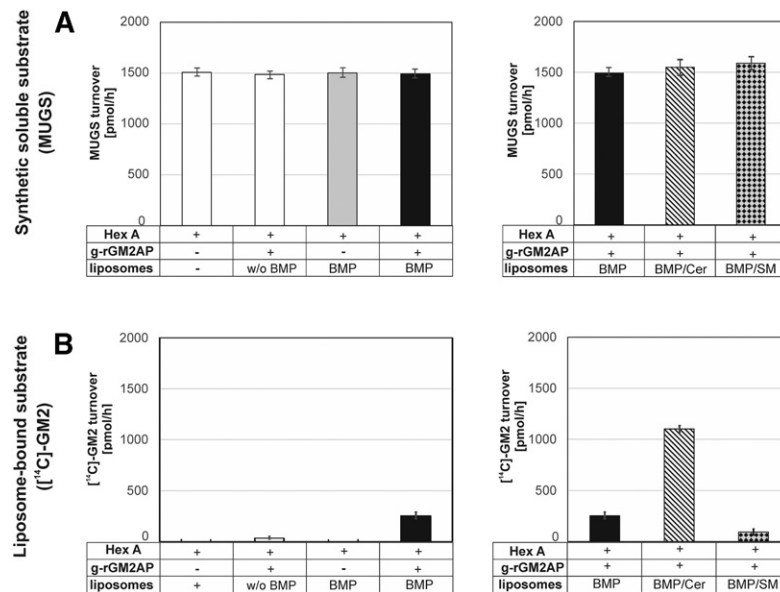
Fig. 1. Hydrolysis of the synthetic, water-soluble substrate MUGS by Hex A (A) and turnover of liposome-bound [^{14}C]GM2 by Hex A in the presence of GM2AP (B). The activity of Hex A is usually determined by an assay using the water-soluble, synthetic substrate MUGS. It is also known that the hydrolysis of the natural membrane-bound GM2 by Hex A occurs only in the presence of GM2AP (17, 23) and strongly depends on the presence of membrane lipids such as BMP, Cer, and SM (23) (B). The highest GM2 turnover was reached in the presence of GM2AP, Cer, and anionic BMP in the liposomal membranes. To investigate the influence of membrane lipids on the digestion of MUGS by Hex A, liposomes containing 5 mol% Chol, 0 or 20 mol% BMP, 0 or 40 mol% Cer and SM, respectively, and DOPC as a host lipid (0.5 mM in 20 mM citrate buffer, pH 4.2) were added to the assay mixture. However, the addition of different liposomes containing additional Cer or SM to the assay mixture had no significant effect on the turnover of MUGS (A, right). In addition, neither GM2AP nor anionic membrane lipids (BMP) influenced the cleavage of the synthetic soluble substrate MUGS by Hex A (A, left). To mimic the conditions at the intralysosomal vesicles, the turnover of membrane-bound GM2 by Hex A in the presence of GM2AP was measured in a liposomal assay system (B). The liposome composition was as given above and contained additional [^{14}C]GM2 (2 mol%) and 0 or 20 mol% BMP. GM2 turnover was inhibited by SM, even in the presence of BMP, and strongly enhanced by Cer (B, right) ($n = 3$).

above the baseline represent material bound to the lipid layer during the experiment, whereas RUs below the baseline represent the loss of lipid material mobilized and released from the lipid layer.

Any increase of RU values indicates binding of additional material (e.g., g-rGM2AP) to the lipid layer, and any drop of RU values indicates the loss of material, GM2AP or lipids, from the sensor chip. For detailed information see the Material and Methods section. The release and mobilization of liposomal lipids have been analyzed previously by using radiolabeled membrane lipids (38).

A dose-dependent inhibitory effect of SM on GM2 hydrolysis by Hex A was obtained in the presence of GM2AP using BMP-containing, negatively charged liposomes (Fig. 2A). It was also observed in BMP-free liposomes (Fig. 3A), while the level of GM2 turnover reached only 12% to 17% of that observed in the case of the much more negatively charged BMP-containing liposomes. SM also retarded the lipid mobilization by g-rGM2AP strongly (Fig. 4A) in a dose-dependent manner. At 30–40 mol% SM in the liposomal preparation, g-rGM2AP bound to the lipid layer but released hardly any material, even when the buffer was injected.

In the late endosomal compartment, Chol is sorted out from the inner endosomal membranes by the proteins NPC1 and NPC2, avoiding the inhibition of GM2 catabolism

(4, 10). High Chol levels inhibited both GM2 hydrolysis and lipid mobilization by GM2AP (Figs. 2B, 3B, 4B), the inhibiting effect was tightened and enhanced by rising Chol concentrations. Using BMP-containing liposomes with an enhanced negative net charge and 40 mol% Chol, the turnover of GM2 was reduced to 30% compared with liposomes containing only 5 mol% Chol (Fig. 2B). A similar effect was also observed using liposomes free of BMP (Fig. 3B), but the amount of hydrolyzed GM2 was only 12% to 20% compared with the GM2 turnover using BMP-containing liposomes.

Enhanced Chol concentration drastically reduced the mobilization of lipids. Introducing 30–40 mol% Chol into the liposomal preparation resulted in an enhanced binding of g-rGM2AP to the lipid layer but prohibited any lipid mobilization (Fig. 4B).

Lysosomal degradation products Cer, DAG, lyso-PC, and stearic acid stimulate GM2 hydrolysis and lipid mobilization by GM2AP

Lysosomal degradation of phospho- and glycolipids generates lipid products such as lyso-PC, DAG, Cer, and fatty acids in the lysosomal compartment. Their influence on GM2 hydrolysis was examined. The stimulating effects of DAG, Cer, stearic acid, and lyso-PC on GM2 hydrolysis in
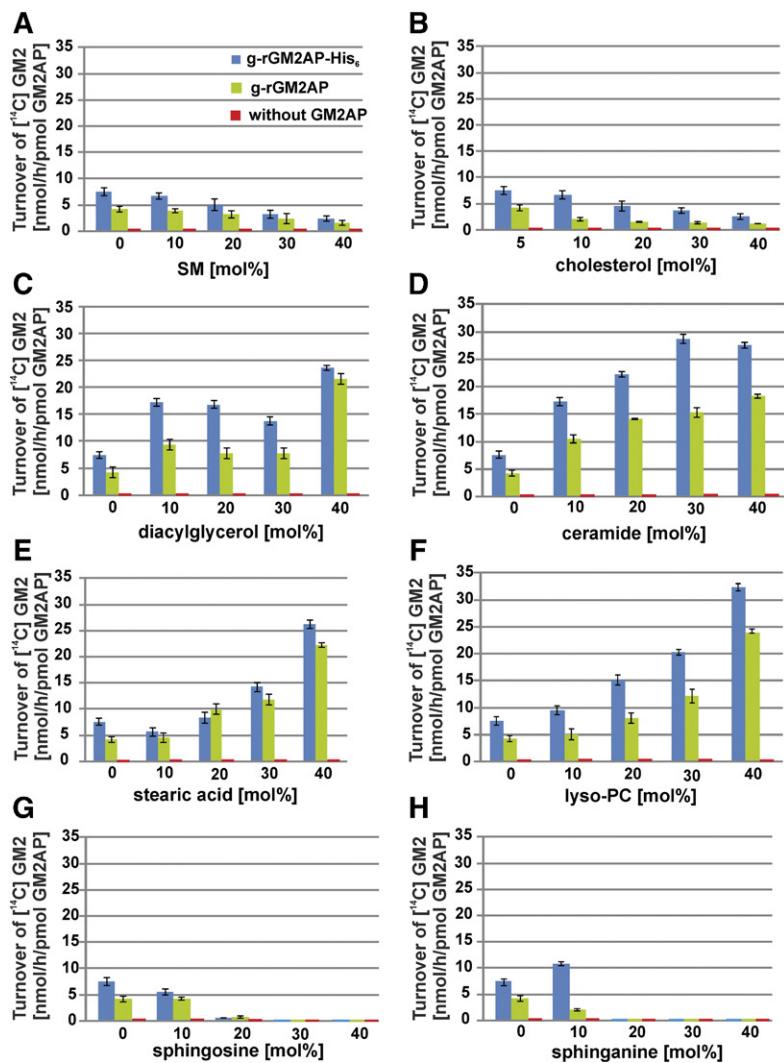
Fig. 2. GM2 hydrolysis is strongly modified by membrane lipids in BMP-containing liposomes. The influence of increasing liposomal concentrations of SM (A), Chol (B), DAG (C), Cer (D), stearic acid (E), lyso-PC (F), So (G), Sa (H) on the conversion of GM2 to GM3 by Hex A in the absence of GM2AP (red), and the presence of g-rGM2AP (green) and g-rGM2AP-His$_6$ (blue) was investigated in an in vitro liposomal assay using negatively charged, BMP-containing liposomes. The liposomal composition was Chol (5 mol%), BMP (20 mol%), lipid of interest (0–40 mol%), and [^{14}C]GM2 (2 mol%), made up to 100 mol% by DOPC. The turnover of [^{14}C]GM2 in the liposomal activity assay was strongly stimulated by DAG (C), Cer (D), stearic acid (E), and lyso-PC (F) and inhibited by SM (A), Chol (B), So (G), or Sa (H). In the absence of GM2AP, no hydrolysis of GM2 was detectable (A–H) ($n = 3$).

negatively charged, BMP-containing, GM2-carrying liposomes are shown in Fig. 2C–F.

Cer arises in the late endosome as a degradation product of SM and glycosphingolipids (19, 22). Whereas SM inhibits GM2 catabolism (Figs. 2A, 3A), Cer stimulates it (Figs. 2D, 3D) (23). The hydrolysis of GM2 was enhanced with heightened concentrations of the lipid of interest. The highest increase of GM2 hydrolysis in the presence of g-rGM2AP was observed in the presence of 40 mol% lyso-PC (enhancement to nearly 6-fold) (Fig. 2F) or stearic acid (enhancement to 5.5-fold), while Cer at 40 mol% was slightly less effective (Fig. 2D).

Though the rate of GM2 hydrolysis using liposomes free of BMP (Fig. 3) was about an order of magnitude lower than in BMP-containing liposomes (Fig. 2), the stimulating effects of DAG, Cer, stearic acid, and lyso-PC could still be detected (Fig. 3C–F). DAG at 40 mol% nearly doubled GM2 hydrolysis by Hex A in the presence of r-gGM2AP (Fig. 3C), while Cer at 40 mol% enhanced GM2 turnover more than 2-fold (Fig. 3D) and lyso-PC at 40 mol% led to a 2.6-fold stimulation of GM2 turnover (Fig. 3F). The catabolism of GM2 by Hex A was always enhanced more effectively when the more protonated g-rGM2AP-His$_6$ was used instead of the naturally occurring g-rGM2AP.

It was also observed that the stimulating lipids DAG, Cer, stearic acid, and lyso-PC facilitate the solubilization and mobilization of membrane lipids by GM2AP (Fig. 4C–F). In control experiments without lipid modifiers (Fig. 4, red lines), the early injection of g-rGM2AP resulted in a slight increase of RUs, corresponding to an absorption of GM2AP at the lipid layer. The RU signal then dropped below the baseline during the injection of g-rGM2AP and continued to descend after the injection of the buffer, indicating the release of membrane lipids (and g-rGM2AP). The addition of DAG (10–40 mol%) resulted in a concentration-dependent acceleration of lipid release but did not enhance the overall amount of lipids released (Fig. 4C). Of the lipid material bound to the chip, 70% was released from the chip in the control experiment. The addition of 30–40 mol% DAG to the liposomal preparation resulted only in a small increase of lipid mobilization up to 75% (Fig. 4C). In the case of 10 mol% Cer, the total amount of mobilized material was extremely reduced to one-third of the control (0 mol% Cer, red line), whereas 20–30 mol% Cer was less inhibitory (Fig. 4D). Cer at 30 mol% resulted in 70% mobilization of lipid material, which was comparable to liposomes free of Cer. Lipid mobilization was slightly enhanced with 40 mol% Cer, resulting in 75 mol% (Fig. 4D).
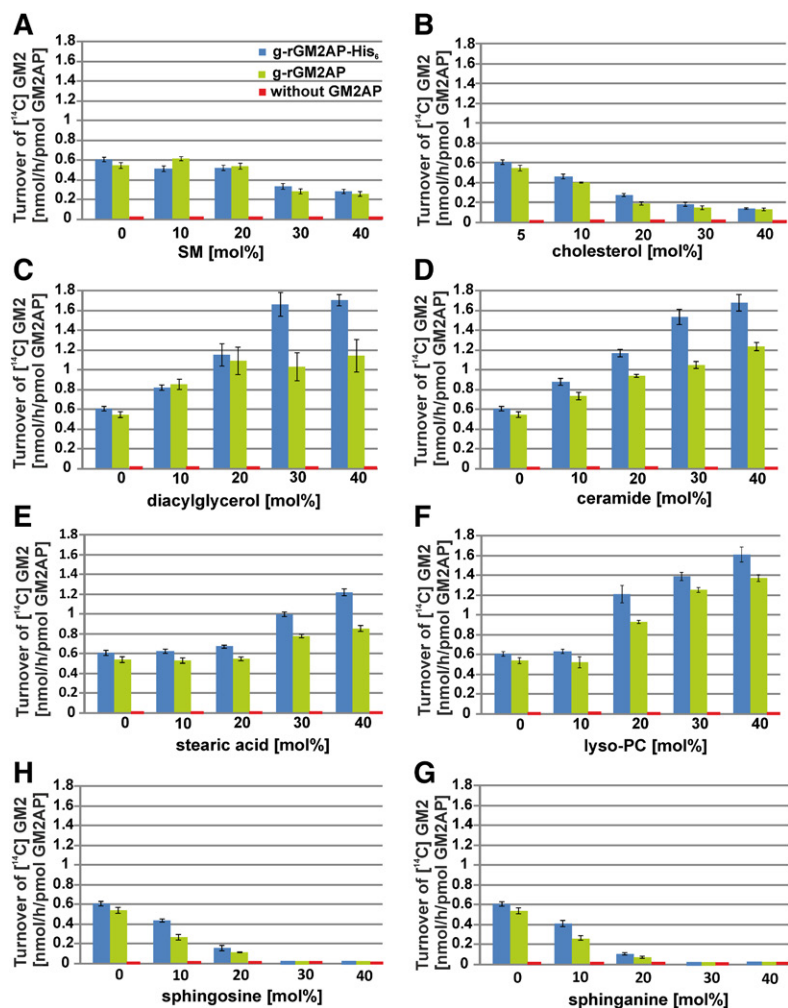
Fig. 3. GM2 digestion is also affected by membrane lipids in BMP-free liposomes. The influence of the liposomal lipids SM (A), Chol (B), DAG (C), Cer (D), stearic acid (E), lyso-PC (F), So (G), and Sa (H) on the conversion of GM2 to GM3 by Hex A in the presence of g-rGM2AP (green) and g-rGM2AP-His$_6$ (blue) was investigated using BMP-free liposomes. The turnover of GM2 was fundamentally reduced compared with liposomes containing 20 mol% BMP and carrying a stronger negative net charge (see Fig. 2). Enhanced liposomal DAG (C), Cer (D), stearic acid (E), or lyso-PC (F) concentrations led to an enhanced hydrolysis of GM2 by Hex A in the presence of g-rGM2AP (green) and g-rGM2AP-His$_6$ (blue) in the in vitro liposomal activity assay (C–F) while increasing SM (A), Chol (B), So (G), and Sa (H) concentrations reduced it (A, B, H, G). In the absence of GM2AP, no hydrolysis of GM2 was detectable (A–H) ($n = 3$).

The addition of stearic acid (10–40 mol%) led to a reduced and concentration-dependent binding of g-rGM2AP to the lipid layer and an accelerated and more complete mobilization of lipids up to 85% of the loaded lipids (Fig. 4E).

Low levels of lyso-PC (10–20 mol%) in the liposomal preparation enhanced the binding of g-rGM2AP to the lipid layer, but the signal did not drop below the baseline until the buffer was injected. After the buffer was injected the signal dropped slightly below the baseline, indicating the mobilization of lipids, but did not reach the level that was achieved using liposomes without lyso-PC. A lyso-PC concentration of 20 mol% resulted in a small amount of released lipids, even before the injection of buffer. Enhancing the lyso-PC concentration to 30 or 40 mol% led to an accelerated mobilization of membrane lipids, indicated by the dropping of the experimental curve below the control line (red), already before the buffer was injected. The final amount of lost material (lipids and proteins) was not enhanced compared with measurements without lyso-PC. So lyso-PC levels (10–20 mol%) reduced lipid mobilization, while higher concentrations (30–40 mol%) mobilized lipids faster compared with the control experiment (red line) (Fig. 4F).

Whereas g-rGM2AP steadily mobilized lipids from BMP-containing liposomes (Fig. 4), it did not mobilize any lipids from BMP-free, less negatively charged lipid layers (**Fig. 5**). Even the incorporation of Cer (0–40 mol%) or stearic acid (0–40 mol%) did not lead to lipid mobilization by g-rGM2AP.

g-rGM2AP bound to the BMP-free lipid layer containing Cer concentrations of 0–40 mol% at an assay pH of 4.2. With the injection of the buffer some amount of the proteins was released, but the signal did not reach or drop below the baseline, indicating no release of lipids (Fig. 5A). The binding of g-rGM2AP to BMP-free liposomes containing stearic acid (0–40 mol%) was slightly reduced by increasing concentrations of the fatty acid. Injecting the buffer resulted in the release of a part of g-rGM2AP. The signal dropped but did not reach the baseline, producing no evidence for the removal of lipids.

Cationic sphingoid bases, stored in Niemann-Pick type C disease, inhibit GM2 hydrolysis and lipid mobilization by GM2AP

The cationic sphingoid bases So and Sa arise in the lysosomal compartment by the degradation of Cer. Their levels are increased in some lysosomal storage disorders such as Niemann-Pick type C disease, in which they are thought to increase the pH value (50–53). The cationic amphiphiles So and Sa turned out to strongly inhibit the catabolism of GM2 by Hex A in the presence of GM2AP using negatively charged liposomes with 20 mol% BMP (Fig. 2G, H). Adding 20–40 mol% So or Sa to the liposomal
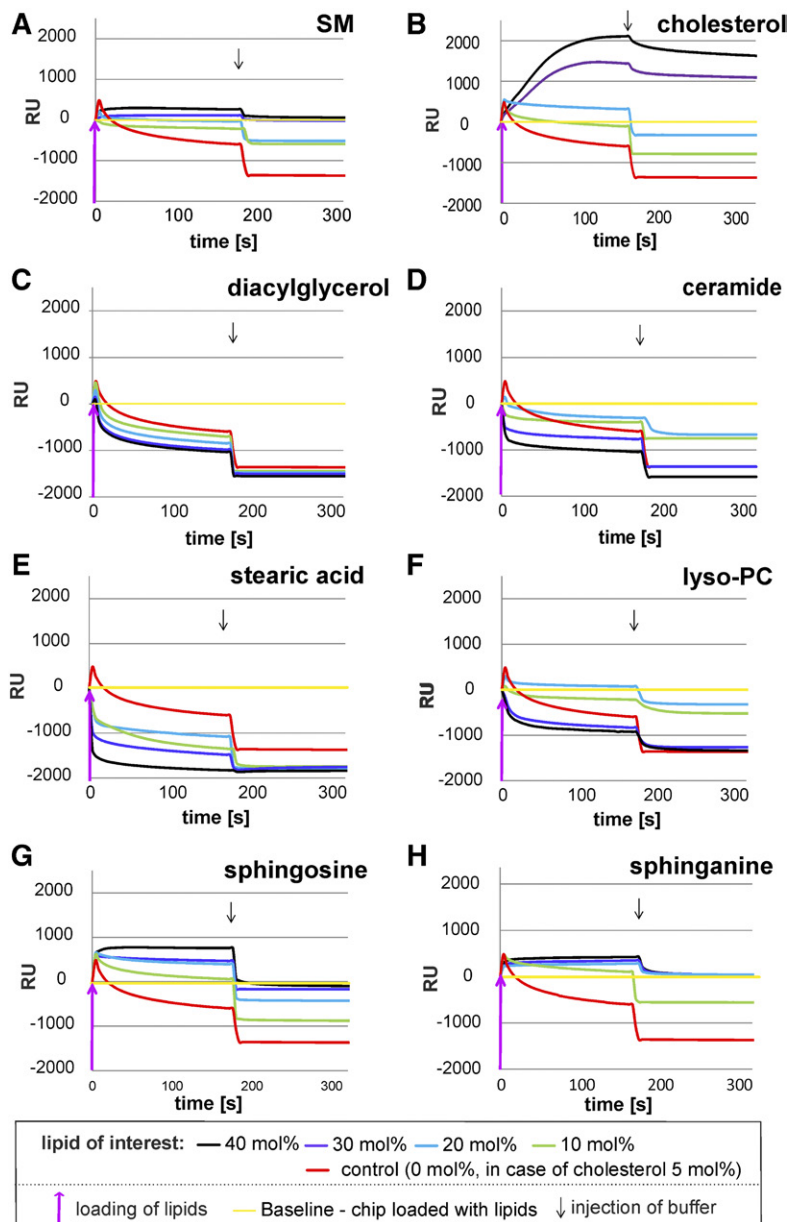
Fig. 4. Mobilization of membrane lipids from BMP-containing, negatively charged lipid layers by GM2AP is strongly modified by the liposomal lipid composition. The binding and mobilization of membrane lipids by g-rGM2AP were investigated in SPR studies. After the immobilization of negatively charged liposomes containing 0–40 mol% lipid of interest, 20 mol% BMP, 5 mol% Chol, 10 mol% GM2, and DOPC as a host lipid, g-rGM2AP was injected into the flow cell (2.5 µM in 20 mM sodium citrate, pH 4.2) at a flow rate of 20 µl/min for 180 s. This was followed by an injection of protein-free buffer (220 s, 20 µl/min), indicated by an arrow. Curves falling below the baseline (yellow) suggest solubilization and mobilization of membrane lipids. Loading of lipids resulted in a shift of approximately 2,000 RUs, which corresponds to a lipid monolayer and was set as the baseline (RU = 0). The baseline corresponds to 100% of loaded lipid material. The RUs above the baseline (yellow) represent material bound to the lipid layer during the experiment, whereas RUs below the baseline represent material loss, which not only includes protein (GM2AP) added during the experiment but also lipid material mobilized and released from the lipid layer. Only if the RU value drops below the baseline can we be certain that lipids from the lipid layer have been removed, in amounts equal to the RU values given. The mobilization of lipids from lipid layers consisting of 0 mol% lipid of interest, 20 mol% BMP, and 5 mol% Chol by g-rGM2AP was set as the control for all experiments (red line). All lines shown are one representative out of three. BMP, DAG, Cer, stearic acid, and lyso-PC stimulated lipid mobilization by GM2AP, while SM, Chol, So, and Sa inhibited it.

membrane blocked the catabolism of GM2 completely, an inhibition that was also observed with liposomes free of BMP (Fig. 3G, H), in which the rate of GM2 hydrolysis was reduced to 6% to 17% compared with BMP-containing liposomes. Similar effects were seen with g-rGM2AP-His$_6$, although the GM2 turnover was always increased compared with experiments with naturally occurring, untagged g-rGM2AP.

In addition, the lipid mobilization was inhibited by So and Sa in a dose-dependent manner. Enhancing the liposomal level of the sphingoid bases So and Sa strongly reduced the mobilization of membrane lipids by g-rGM2AP. Adding 30–40 mol% So to the liposomal formulation g-rGM2AP bound strongly to the lipid layer. After the buffer was injected, the protein dissolved, dropping slightly below the baseline, suggesting a minor mobilization of membrane lipids (Fig. 4G). When 30–40 mol% Sa was used, g-rGM2AP bound to the membrane layer, dissolved when the buffer was added, but did not drop below the baseline (Fig. 4H).

The six histidine residues at the C-terminal end of g-rGM2AP-His$_6$ do not only have a strong influence on the hydrolysis of GM2 by Hex A using various lipid compositions. The His$_6$-tag also inhibited the mobilization of membrane lipids by GM2AP, as observed previously (23). Because of the unnatural behavior of the His$_6$-tagged protein, we did not use it for SPR studies.

DISCUSSION

Membrane lipids play a central role as regulators and modifiers of cellular functions mediated by the plasma membrane and organellar membranes. The specific composition of subcellular membranes, including their lipid pattern, is significant for the function of membrane properties (54), e.g., a high concentration of Chol in the plasma membrane for the regulation of Na$^+$, K$^+$-ATPase (55).

Whereas Chol and SM stabilize the plasma membrane, they are inhibitory for some key reactions in lysosomal
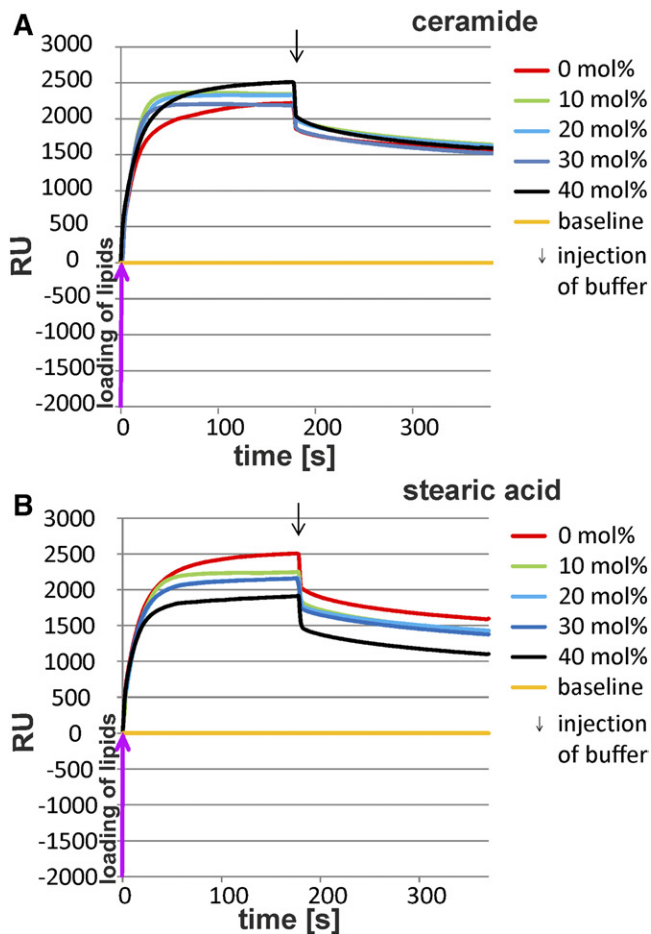
Fig. 5. GM2AP could not mobilize lipids from BMP-free lipid layers. The mobilization of membrane lipids by g-rGM2AP was investigated in SPR studies. Conditions were equal to that of Fig. 4. Liposomes did not contain BMP.

glycosphingolipid catabolism (6). On the other hand, the catabolism of (glyco)sphingolipids such as GM2 (17, 23), GM1 (18), sulfatide (21), glycosylceramide (25), Cer (19), SM (22), and phospholipids (56) is extremely enhanced by anionic lipids such as BMP at lysosomal pH values, mainly due to an electrostatic binding of protonated cationic lysosomal proteins to the negatively charged membranes of the liposomes and the ILVs carrying the (glyco)sphingolipid to be digested. The ILVs are enriched with BMP and may contain other anionic phospholipids that carry a negative charge at low pH values, resulting in a negative zeta potential of the ILV membranes (22). The conditions at the ILVs in the lysosome are illustrated in **Fig. 6**.

Disturbed lysosomal sphingolipid degradation, often caused by an inherited hydrolase deficiency, results in lysosomal storage disorders, a group of at least 40 hereditary diseases. In most of these disorders indigestible primary storage compounds accumulate besides others, presumably secondary storage compounds (57).

In this study we examined the regulatory and modifying influence of some primary storage compounds and a multitude of membrane lipids and their degradation products on the catabolism of membrane-bound GM2 by Hex A assisted by GM2AP compared with their influence on the

turnover of the synthetic, water-soluble substrate MUGS by Hex A, often used to assay Hex A activity in patients with lysosomal storage disorders.

The addition of increasing concentrations of bilayer-destroying lipids to the liposomal membranes, fatty acids, sphingoid bases (Sa, So), and DAG, however, may well generate other lipid aggregates than lipid bilayer liposomes, e.g., lipid layers, aggregates, or micelles. However, this would also apply to ILVs in the living cells that incorporate those lipids released as intermediates of lipid catabolism at higher concentrations.

Membrane lipids and their degradation compounds regulate GM2 hydrolysis and lipid mobilization by GM2AP but do not affect Hex A-catalyzed hydrolysis of soluble synthetic substrates

The GM2-cleaving Hex A is a promiscuous glycosidase, hydrolyzing a multitude of soluble β-*N*-acetyl-glucosaminides and -galactosaminides, e.g., oligosaccharides, mucopolysaccharides, glycolipids, and synthetic soluble substrates such as MUGS (44, 58). Though Hex A can attack soluble substrates such as MUGS directly, soluble Hex A does not recognize amphiphilic, membrane-bound substrates such as GM2 in the absence of the cofactor GM2AP (42, 59, 60), but it interacts with the stoichiometric GM2-GM2AP complex as a substrate, forming a Michaelis-Menten complex (61) (Fig. 6A). The inherited absence of GM2AP causes GM2 storage in the AB variant of GM2 gangliosidoses (62, 63).

Hex A shows a broad pH profile (3.0–7.6) against soluble synthetic substrates (42) but a sharp one (3.8–4.6) for the cleavage of membrane-bound amphiphilic GM2 in the presence of its cofactor GM2AP (15, 17, 23, 64). In contrast to MUGS hydrolysis, the cleavage of membrane-bound liposomal GM2 depends completely on the cofactor protein GM2AP and the lipid composition of the liposomal membrane (Figs. 2, 3) (17, 23). In contrast to the catabolism of membrane-bound GM2, the main storage compound of GM2 gangliosidoses (Tay-Sachs disease, Sandhoff disease, and the AB or B1 variants of GM2 gangliodosis), the cleavage of soluble synthetic substrates such as MUGS is hardly affected by the presence of GM2AP and membrane lipids present in the form of liposomes, lipid aggregates, or detergent micelles (Fig. 1).

In addition, stabilizing lipids of the plasma membrane, Chol and SM, and its final lysosomal degradation products, Sa and So, strongly inhibit the catabolism of liposomal-bound GM2 (Figs. 2A, B, G, H, 3A, B, G, H) but not that of soluble MUGS (data not shown). Whereas several intermediates of lysosomal lipid degradation (DAG, Cer, fatty acids, and lyso-PC) stimulate enzymatic hydrolysis of liposomal-bound GM2 up to 5-fold (Figs. 2C–F, 3C–F), they do not affect that of soluble MUGS (Fig. 1).

In summary, lipid modifiers mainly affect the functions of the GM2AP at the membrane surface, the electrostatic binding of proteins to the surface of the GM2-containing membranes, the mobilization of membrane lipids by GM2AP (Fig. 4), and the GM2AP-dependent Hex A-catalyzed GM2 hydrolysis (Figs. 2, 3). They may also affect the Michaelis-Menten complex formation (GM2-GM2AP-Hex A) directly,
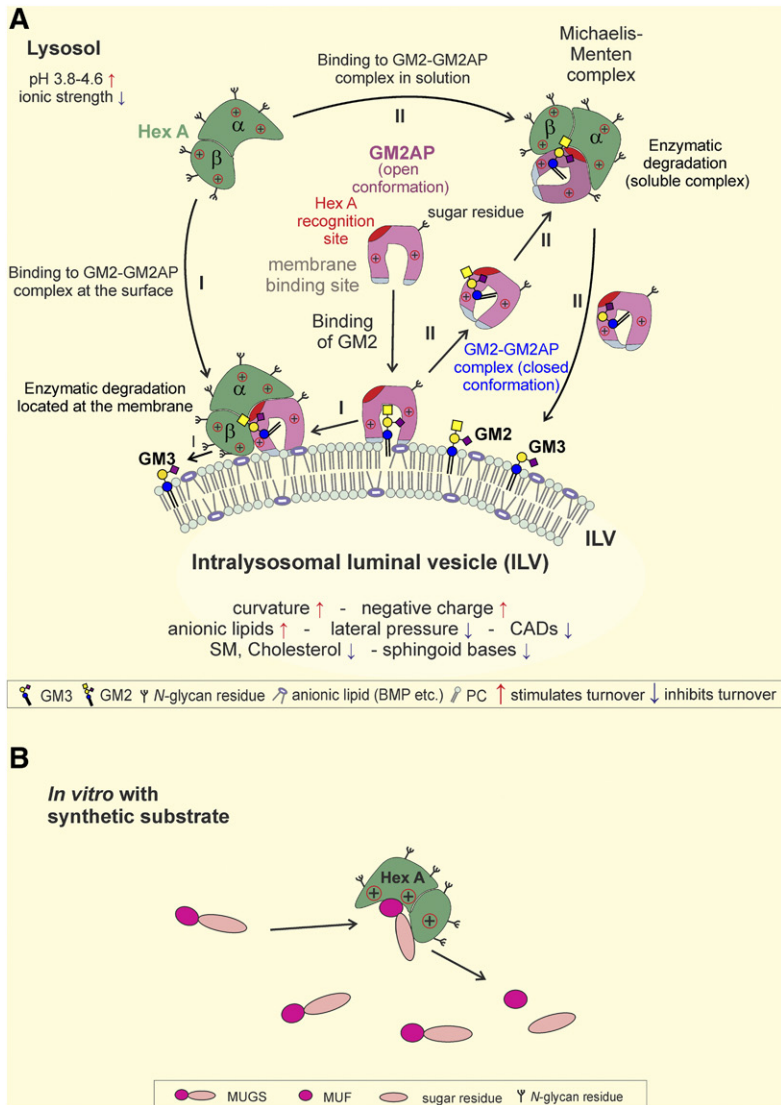
Fig. 6. Enzymatic hydrolysis of membrane-bound ganglioside GM2 by Hex A in the presence of GM2AP (A) and turnover of the soluble substrate MUGS by Hex A (B). A: Model for the hydrolysis of membrane-bound GM2 by Hex A, assisted by GM2AP, at the surface of luminal lysosomal vesicles. Assisted by the hydrophobic loops (bluish gray), the GM2AP can bind to the membrane and penetrates into the hydrophobic region of the bilayer. Its hydrophobic cavity can include the Cer tail of GM2 and other lipids (61) and stay at the membrane (I). The conformation of the lipid GM2AP complex can also change to a more closed conformation, thus becoming more water-soluble, and detach from the lipid layer as a water-soluble Michaelis-Menten-complex (II), exposing the GM2 to the water-soluble Hex A for degradation. Hydrolysis of GM2 by Hex A assisted by GM2AP is based on a pH level from 3.8 to 4.6 combined with a low ionic strength (23, 39). It is enhanced by the membrane curvature of the ILVs and a negative charge due to anionic lipids such as BMP. However, high lateral pressure, CADs, SM, Chol, and sphingoid bases reduce GM2 hydrolysis. Modified from (5, 6). B: In vitro Hex A can cleave the synthetic substrate MUF without assistance from auxiliary proteins. The turnover of MUGS to MUF is unaffected by the regulatory system involved in the lysosomal turnover of GM2 by Hex A and GM2AP shown in panel A.

but they do not affect the Hex A-catalyzed hydrolysis of synthetic, water-soluble substrates such as MUGS.

Electrostatic interactions between protonated lysosomal proteins and negatively charged ILVs

At low pH values (e.g., 4–4.8), most lysosomal proteins, hydrolases, and sphingolipid activator proteins are positively charged and concentrate on the surface of lipid substrate-carrying, negatively charged ILVs to speed up lipid hydrolysis at the vesicle surface (22, 23).

In reconstitution experiments, liposomes containing 20 mol% BMP or other anionic phospholipids (phosphatidylglycerol, phosphatidylinositol, phosphatic acid) carry a negative zeta potential at their surface (22). This negative surface charge of ILVs should attract and concentrate positively charged proteins such as acid sphingomyelinase (22, 65), glucocerebrosidase (25), and other hydrolases and sphingolipid activator proteins such as GM2AP (23, 38, 66) at their surface. Due to the additional protonation of the His_6-tag at low pH values, the electrostatic attraction of His_6-tagged sphingolipid activator proteins such as g-rGM2AP-His_6 is further enhanced to the GM2-carrying vesicular surface

and leads to a stronger concentration at the vesicular surface and an increase of the catabolic reaction rate (Figs. 2, 3). On the other hand, cationic amphiphilic drugs added to the assay (or fed to cultured fibroblasts) (65, 67) can compensate for the negative surface charge and trigger the release of vesicle-bound proteins, thereby reducing sphingolipid and glycosphingolipid catabolism (65, 67). The release of ILV-bound lysosomal hydrolases can also facilitate their proteolytic digestion in the lysosomes and trigger a drug-induced lipidosis (65, 67).

Enhancement of GM2 turnover by the removal of inhibiting membrane lipids from ILVs and generation of modifying lipid intermediates

The plasma membrane-stabilizing lipids Chol and SM inhibit several key steps in sphingolipid catabolism (7) (Figs. 2A, B, 3A, B). The conversion of inhibiting SM to stimulating Cer at ILVs of late endosomes facilitates the removal of Chol by NPC2 from the ILVs and stimulates the catabolism of several sphingolipids (22).

The action of the promiscuous phospholipase C, the acid sphingomyelinase, and the lysosomal phospholipase

A2 will generate a series of degradation products, DAG, Cer, fatty acids, and lyso-PC (68–70). In addition, those early degradation products of phospholipids and sphingolipids such as DAG, Cer, fatty acids, and lyso-PC will disturb the bilayer structures of ILVs and create lipid micelles and aggregates in the lumen of the lysosomes that can be digested much faster by lysosomal lipases and glycosidases than the lipids in the vesicular membranes.

DAGs can accumulate transiently in membranes and cause changes in the physical properties of the bilayer. They tend to form inverted micellar structures because their polar head group is small. This leads to the formation of small areas of unstable negative curvature in membranes that facilitate membrane fission and fusion (71, 72).

It is known that Cer induces transbilayer flip-flop (73), induces membrane efflux from large unilamellar vesicles, and creates Cer-rich domains in plasma membranes (74, 75). Its strong stimulation of GM2 turnover may also be based on its bilayer-labilizing abilities.

The micelle-forming lipid lyso-PC can be generated in the lysosome as an intermediate of phosphatidylcholine catabolism. Formed in ILVs, it may well labilize the stability of ILV membranes, thereby stimulating GM2 and lipid mobilization. Stearic acid induces the formation of micelles and due to its negative surface charge at slightly acidic conditions facilitates lipid degradation by soluble and protonated lysosomal enzymes.

The bilayer-disturbing lipids DAG, Cer, stearic acid, and lyso-PC elevated the GM2 turnover in a concentration-dependent manner, using BMP-containing liposomes with an enhanced negative surface charge (Fig. 2C–F). This influence was also observed in BMP-free liposomes, exhibiting, however, rather low metabolic rates due to an extremely reduced negative surface charge (Fig. 3C–F). Similar effects had been observed before concerning the turnover of glycosylceramide (25) and other glycosphingolipids. Moreover, DAG has been described to act as a stimulator for acid sphingomyelinase (22, 76). Its stimulatory effects on SM and GM2 hydrolysis may be based on its bilayer-perturbing properties. They may be also responsible for the slightly stimulating effects on lipid mobilization as observed in SPR studies (Fig. 4C).

The potent stimulatory impact of the micelle-forming stearic acid on GM2 hydrolysis and lipid mobilization may be based on its cone-shaped form, having a voluminous hydrated head group and a single hydrophobic chain. With a pK value of about 4.8, its stimulatory impact may also be increased by a small percentage of still unprotonated and negatively charged stearic acid molecules at the pH range of GM2 hydrolysis of 3.8 to 4.6 (39).

In addition, of all lipids mentioned above, only micelle-forming stearic acid had a strong stimulating effect on lipid mobilization by g-rGM2AP in SPR studies (Fig. 4C–F). This observation may also be very important for other lipid bilayer-disturbing and micelle-forming fatty acids that are released in large amounts by triacylglycerol and phospholipid catabolism in the lysosomal system.

SM is reported to stabilize Chol in the membrane by shielding its OH−group (77). During the maturation of ILVs SM is degraded to Cer (78, 79). As in previous experiments (23), we could show that the zwitterionic and bilayer-stabilizing SM inhibits the GM2AP dependent GM2 hydrolysis, even in the presence of the stimulating lysosomal lipid BMP (2, 17, 38) (Fig. 2A). This is supported by the strong inhibition of g-rGM2AP-mediated lipid mobilization by SM-containing membranes (Fig. 4A).

Chol is the major steroid constituent of mammalian membranes. It has membrane-stabilizing properties, enables the lipid-ordered phase of lipid bilayer structures, and reduces the membrane permeability for ions (55, 80, 81). During endocytosis, the Chol content decreases in the intraendolysosomal vesicles. It is sorted out by the sterol binding proteins NPC1 and NPC2 (4, 7, 22, 82, 83). As shown previously (23), Chol is a strong inhibitor for the hydrolysis of GM2 (Figs. 2B, 3B). It triggers GM2 accumulation in Niemann-Pick type C disease and inhibits lipid mobilization by g-rGM2AP (Fig. 4B), even in the presence of the stimulating lysosomal lipid BMP (2, 17, 38).

So and Sa are two free sphingoid bases whose pathomechanisms have been reviewed previously (84). They are highly cytotoxic and closely associated to the primary defects in Krabbe disease, Fabry disease, and Niemann-Pick disease (53, 85–87). They are strong inhibitors of glycosylceramide hydrolysis (25, 88), presumably due to their positive net charge. As components of the lipid substrate-carrying membrane they reduce the electrostatic interaction between the cationic enzyme or protein and the negatively charged membrane surface (88). It is postulated that they act in a similar way as cationic amphiphilic drugs (CADs) inducing a lipidosis. Like desipramine (65) they may trigger a dissociation of acid spingomyelinase and other hydrolases from the lipid layers, thereby reducing the catabolic rates. Even low concentrations of amphiphilic amines e.g., So and the CAD imipramine can provoke an "NPC phenotype" (89). Indeed, So and Sa have strong inhibitory influence on GM2 turnover (Fig. 2G, H), as seen previously for glycosylceramide catabolism (25). They also strongly inhibit lipid mobilization by GM2AP, as seen in SPR studies (Fig. 4G, H). Levels of sphingoid bases in the lysosomal compartment are mostly unknown, but they may well increase in lysosomes, especially when their egress is impaired by storage material.

Severe side effects of the His$_6$-tag

The His$_6$-tag was added to recombinant GM2AP to enable its simple purification. At lysosomal pH values the increased cationic charge of the His$_6$-tagged GM2AP, however, may enhance its electrostatic binding to the negatively charged surface of BMP-containing liposomes and ILVs. This may well increase the GM2AP concentration at the substrate-carrying vesicle surfaces and thereby enhance the Hex A-mediated GM2 hydrolysis in the in vitro activity assay, as observed in Figs. 3 and 4. The GM2 turnover-enhancing effect of the His$_6$-tag is independent of the vesicle formulation in the activity assays (Figs. 2A–H, 3A–H) and seems to be based on the additional positive charge of the six additional histidine residues protonated at low pH values that should result in a stronger electrostatic binding to the negatively charged liposomal membrane. Based on

these findings we postulate that the hydrolysis of GM2 by Hex A in the presence of g-rGM2AP-His$_6$ takes place at the membrane surface and not in solution, leading to the conclusion that His$_6$-tagged membrane active proteins should not be used in reconstitution assays.

As mentioned previously (23), the His$_6$-tag has more than one side effect on the overall properties of GM2AP. It enhances turnover of GM2 by Hex A, assisted by GM2AP; speeds up the intermembrane lipid transfer of 2-NBD-GM1 in Förster resonance energy transfer studies; and inhibits lipid mobilization by GM2AP in SPR studies (23).

CONCLUSIONS

In this study, we characterized the impact of various membrane lipids on the GM2 catabolism at and in the ILVs. Primary GM2 storage is known to be based on mutations in the α and β Hex A subunits (Tay Sachs disease and Sandhoff disease) and in the GM2 activator (AB variant). Here, the influence of changes in ILV lipid composition on GM2 catabolism as a regulator of GM2 turnover, possibly also affecting lysosomal storage, has been less illuminated. We present clear evidence that Chol and SM as well as the lysosomal degradation compounds So and Sa could inhibit GM2AP-assisted GM2 hydrolysis by Hex A. Furthermore, the incorporation of Cer, DAG, fatty acids, and lyso-PC into the GM2-carrying membrane could stimulate it. In contrast to the altered activities of GM2AP-assisted GM2 catabolism, the Hex A-catalyzed hydrolysis of the synthetic, water-soluble substrate MUGS was not affected by all lipid alterations. These findings may provide an explanation for secondary GM2 storage as a consequence of lipid alterations induced by lysosomal storage disorders.

Posttranscriptional and posttranslational generated compounds and other cofactors in the microenvironment of the substrate-carrying membranes regulate and modify the lipid-cleaving activity of catabolic lysosomal hydrolases effectively, in contrast to the hydrolysis of soluble synthetic substrates such as MUGS. In addition to known factors such as pH, the nature of the substrate (15, 23, 39), ionic strength (23) etc., the GM2AP-assisted hydrolysis of GM2 is influenced by the membrane lipids (23) comprised in the ILVs and by storage compounds of lysosomal storage diseases (90) that can trigger a secondary lipid accumulation and affect pathogeneses in patients. We also found a clinical phenotype correlation between patients with GM2 gangliosidosis and metachromatic leukodystrophy and the sphingolipid-degrading activity of their cultured fibroblasts (91, 92). Lipid-cleaving activity of hydrolases appears to be strongly modified by the molecular microenvironment of the reaction (22). Membrane properties might also be important for the rate of sphingolipid catabolism in the lysosomes. Lateral pressure [as assigned for GM2AP action (93)] and curvature [as demonstrated for Cer (94)] of the vesicle membranes are important but will be only of transient influence. The fast generation of lipid bilayer-destroying catabolic products such as the massive release of micelle-forming free fatty acids by the degradation of tri- and diglycerides, sphingolipids, and phospholipids and the generation of lyso-sphingolipids and lyso-phospholipids will rapidly destroy the membrane bilayer structure of the ILVs and generate a multitude of micelles and other lipid aggregates within the lysosomes. They will be a much better prey for enzymatic catabolism than lipid components of intact membrane structures. This became obvious when comparing in vitro studies of micellar with membrane-bound sulfatides and ganglioside GM2, respectively (95), as substrates of catabolic hydrolases. In addition, the inhibiting action of CADs (90) and sphingoid bases will change with the disappearance of intact membrane structures. Lysosomal storage of ILV membranes is not only massive in inherited defects of lysosomal hydrolases and sphingolipid activator proteins but also becomes prominent in healthy animals after being fed massive amounts of CADs (96, 97) or excessive amounts of lipids and other nutrients. Under normal conditions healthy tissues hardly show any ILV structures. Those are apparently readily degraded (98–100).

Therefore, we postulate that membrane lipids of organellar membranes modify the activity of many organellar proteins. Pathological alterations of their lipid composition may interfere with cellular metabolism (e.g., with the lipid and membrane metabolism in obesity, Alzheimer's disease, and Parkinson's disease). Therefore, the lipid pattern of organelles should be analyzed in situ as soon as appropriate technology will be available with sufficiently high spatial and temporal resolution. Lipidomics of tissues and cells is of only limited value. Though the overall Chol content in the brain appears to be normal, a slight Chol increase in the endosomes and lysosomes is fatal for the patients with Niemann-Pick disease type C (84, 101, 102).

REFERENCES

1. Sandhoff, K., and T. Kolter. 1996. Topology of glycosphingolipid degradation. *Trends Cell Biol.* **6:** 98–103.
2. Matsuzawa, Y., and K. Y. Hostetler. 1979. Degradation of bis(monoacylglycero)phosphate by an acid phosphodiesterase in rat liver lysosomes. *J. Biol. Chem.* **254:** 5997–6001.
3. Möbius, W., E. van Donselaar, Y. Ohno-Iwashita, Y. Shimada, H. F. Heijnen, J. W. Slot, and H. J. Geuze. 2003. Recycling compartments and the internal vesicles of multivesicular bodies harbor most of the cholesterol found in the endocytic pathway. *Traffic.* **4:** 222–231.
4. Wang, M. L., M. Motamed, R. E. Infante, L. Abi-Mosleh, M. S. Brown, and J. L. Goldstein. 2010. Identification of surface residues on Niemann-Pick C2 essential for hydrophobic handoff of cholesterol to NPC1 in lysosomes. *Cell Metab.* **12:** 166–173.
5. Breiden, B., and K. Sandhoff. 2018. Ganglioside metabolism and its inherited diseases. *Methods Mol. Biol.* **1804:** 97–141.
6. Sandhoff, R., and K. Sandhoff. 2018. Emerging concepts of ganglioside metabolism. *FEBS Lett.* **592:** 3835–3864.
7. Abdul-Hammed, M., B. Breiden, M. A. Adebayo, J. O. Babalola, G. Schwarzmann, and K. Sandhoff. 2010. Role of endosomal membrane lipids and NPC2 in cholesterol transfer and membrane fusion. *J. Lipid Res.* **51:** 1747–1760.
8. Ikonen, E. 2008. Cellular cholesterol trafficking and compartmentalization. *Nat. Rev. Mol. Cell Biol.* **9:** 125–138.
9. Hölttä-Vuori, M., R. L. Uronen, J. Repakova, E. Salonen, I. Vattulainen, P. Panula, Z. Li, R. Bittman, and E. Ikonen. 2008.

BODIPY-cholesterol: A new tool to visualize sterol trafficking in living cells and organisms. *Traffic.* **9:** 1839–1849.

10. Gallala, H. D., and K. Sandhoff. 2011. Biological function of the cellular lipid BMP-BMP as a key activator for cholesterol sorting and membrane digestion. *Neurochem. Res.* **36:** 1594–1600.

11. Ferlinz, K., T. Linke, O. Bartelsen, M. Weiler, and K. Sandhoff. 1999. Stimulation of lysosomal sphingomyelin degradation by sphingolipid activator proteins. *Chem. Phys. Lipids.* **102:** 35–43.

12. Lansmann, S., C. G. Schuette, O. Bartelsen, J. Hoernschemeyer, T. Linke, J. Weisgerber, and K. Sandhoff. 2003. Human acid sphingomyelinase. *Eur. J. Biochem.* **270:** 1076–1088.

13. Kolter, T., and K. Sandhoff. 1998. Enzymology of lysosomal glycolipid catabolism. *Trends Glycosci. Glycotechnol.* **10:** 455–468.

14. Sandhoff, K., T. Kolter, and K. Harzer. 2001. Sphingolipid activator proteins. *In* The Metabolic and Molecular Basis of Inherited Disease. C. Scriver, A. L. Beaudet, W. S. Sly, and D. Valle, editors. McGraw-Hill, New York. 3371–3389.

15. Conzelmann, E., and K. Sandhoff. 1979. Purification and characterization of an activator protein for the degradation of glycolipids GM2 and GA2 by hexosaminidase A. *Hoppe Seylers Z. Physiol. Chem.* **360:** 1837–1849.

16. Conzelmann, E., and K. Sandhoff. 1987. Activator proteins for lysosomal glycolipid hydrolysis. *Methods Biochem. Anal.* **32:** 1–23.

17. Werth, N., C. G. Schuette, G. Wilkening, T. Lemm, and K. Sandhoff. 2001. Degradation of membrane-bound ganglioside GM2 by beta-hexosaminidase A. Stimulation by GM2 activator protein and lysosomal lipids. *J. Biol. Chem.* **276:** 12685–12690.

18. Wilkening, G., T. Linke, G. Uhlhorn-Dierks, and K. Sandhoff. 2000. Degradation of membrane-bound ganglioside GM1. Stimulation by bis(monoacylglycero)phosphate and the activator proteins SAP-B and GM2- AP. *J. Biol. Chem.* **275:** 35814–35819.

19. Linke, T., G. Wilkening, F. Sadeghlar, H. Mozcall, K. Bernardo, E. Schuchman, and K. Sandhoff. 2001. Interfacial regulation of acid ceramidase activity. Stimulation of ceramide degradation by lysosomal lipids and sphingolipid activator proteins. *J. Biol. Chem.* **276:** 5760–5768.

20. Wilkening, G., T. Linke, and K. Sandhoff. 1998. Lysosomal degradation on vesicular membrane surfaces. Enhanced glucosylceramide degradation by lysosomal anionic lipids and activators. *J. Biol. Chem.* **273:** 30271–30278.

21. Matzner, U., B. Breiden, G. Schwarzmann, A. Yaghootfam, A. L. Fluharty, A. Hasilik, K. Sandhoff, and V. Gieselmann. 2009. Saposin B-dependent reconstitution of arylsulfatase A activity in vitro and in cell culture models of metachromatic leukodystrophy. *J. Biol. Chem.* **284:** 9372–9381.

22. Oninla, V. O., B. Breiden, J. O. Babalola, and K. Sandhoff. 2014. Acid sphingomyelinase activity is regulated by membrane lipids and facilitates cholesterol transfer by NPC2. *J. Lipid Res.* **55:** 2606–2619.

23. Anheuser, S., B. Breiden, G. Schwarzmann, and K. Sandhoff. 2015. Membrane lipids regulate ganglioside GM2 catabolism and GM2 activator protein activity. *J. Lipid Res.* **56:** 1747–1761.

24. Hepbildikler, S. T., M. Wendeler, R. Sandhoff, and K. Sandhoff. 2003. Interaction of the GM2 activator protein with sulfated and sialylated glycosphingolipids. *Methods Enzymol.* **363:** 207–222.

25. Abdul-Hammed, M., B. Breiden, G. Schwarzmann, and K. Sandhoff. 2017. Lipids regulate the hydrolysis of membrane bound glucosylceramide by lysosomal beta-glucocerebrosidase. *J. Lipid Res.* **58:** 563–577.

26. Trombetta, E. S., M. Ebersold, W. Garrett, M. Pypaert, and I. Mellman. 2003. Activation of lysosomal function during dendritic cell maturation. *Science.* **299:** 1400–1403.

27. Ohkuma, S., and B. Poole. 1978. Fluorescence probe measurement of the intralysosomal pH in living cells and the perturbation of pH by various agents. *Proc. Natl. Acad. Sci. USA.* **75:** 3327–3331.

28. Hama, Y., Y. T. Li, and S. C. Li. 1997. Interaction of GM2 activator protein with glycosphingolipids. *J. Biol. Chem.* **272:** 2828–2833.

29. Wendeler, M., J. Hoernschemeyer, M. John, N. Werth, M. Schoeniger, T. Lemm, R. Hartmann, H. Kessler, and K. Sandhoff. 2004. Expression of the GM2-activator protein in the methylotrophic yeast Pichia pastoris, purification, isotopic labeling, and biophysical characterization. *Protein Expr. Purif.* **34:** 147–157.

30. Meier, E. M., G. Schwarzmann, W. Fürst, and K. Sandhoff. 1991. The human GM2 activator protein. A substrate specific cofactor of beta-hexosaminidase A. *J. Biol. Chem.* **266:** 1879–1887.

31. Schröder, M., D. Schnabel, K. Suzuki, and K. Sandhoff. 1991. A mutation in the gene of a glycolipid-binding protein (GM2 activator) that causes GM2-gangliosidosis variant AB. *FEBS Lett.* **290:** 1–3.

32. Taniguchi, M., Y. Shinoda, H. Ninomiya, M. T. Vanier, and K. Ohno. 2001. Sites and temporal changes of gangliosides GM1/GM2 storage in the Niemann-Pick disease type C mouse brain. *Brain Dev.* **23:** 414–421.

33. Sato, M., S. Akaboshi, T. Katsumoto, M. Taniguchi, K. Higaki, T. Tai, H. Sakuraba, and K. Ohno. 1998. Accumulation of cholesterol and GM2 ganglioside in cells cultured in the presence of progesterone: an implication for the basic defect in Niemann-Pick disease type C. *Brain Dev.* **20:** 50–52.

34. Neufeld, E. F., and J. Muenzer. 2001. The mucopolysaccharidoses. *In* The Metabolic and Molecular Basis of Inherited Disease. C. Scriver, A. L. Beaudet, W. S. Sly, and D. Valle, editors. McGraw-Hill, New York. 3421–3452.

35. Schwarzmann, G., and K. Sandhoff. 1987. Lysogangliosides: synthesis and use in preparing labeled gangliosides. *Methods Enzymol.* **138:** 319–341.

36. Schütte, C. 1999. Strukturuntersuchungen an β-Hexosaminidase B und GM2-Aktivatorprotein durch Proteinchemische Methoden und MALDI-Massenspektrometrie. PhD Thesis: University of Bonn, Bonn, Germany. German.

37. MacDonald, R. C., R. I. MacDonald, B. P. Menco, K. Takeshita, N. K. Subbarao, and L. R. Hu. 1991. Small-volume extrusion apparatus for preparation of large, unilamellar vesicles. *Biochim. Biophys. Acta.* **1061:** 297–303.

38. Remmel, N., S. Locatelli-Hoops, B. Breiden, G. Schwarzmann, and K. Sandhoff. 2007. Saposin B mobilizes lipids from cholesterol-poor and bis(monoacylglycero)phosphate-rich membranes at acidic pH. Unglycosylated patient variant saposin B lacks lipid-extraction capacity. *FEBS J.* **274:** 3405–3420.

39. Bierfreund, U., T. Lemm, A. Hoffmann, G. Uhlhorn-Dierks, R. A. Childs, C. T. Yuen, T. Feizi, and K. Sandhoff. 1999. Recombinant GM2-activator protein stimulates in vivo degradation of GA2 in GM2 gangliosidosis AB variant fibroblasts but exhibits no detectable binding of GA2 in an in vitro assay. *Neurochem. Res.* **24:** 295–300.

40. Guetta, E., and L. Peleg. 2008. Rapid detection of fetal Mendelian disorders: Tay-Sachs disease. *Methods Mol. Biol.* **444:** 147–159.

41. Mistri, M., P. M. Tamhankar, F. Sheth, D. Sanghavi, P. Kondurkar, S. Patil, S. Idicula-Thomas, S. Gupta, and J. Sheth. 2012. Identification of novel mutations in HEXA gene in children affected with Tay Sachs disease from India. *PLoS One.* **7:** e39122.

42. Sandhoff, K., K. Harzer, W. Wassle, and H. Jatzkewitz. 1971. Enzyme alterations and lipid storage in three variants of Tay-Sachs disease. *J. Neurochem.* **18:** 2469–2489.

43. Kolter, T., and K. Sandhoff. 2000. Lysosomal degradation of glycolipids. *In* Carbohydrates in Chemistry and Biology. B. Ernst, G. W. Hart, and P. Sinay, editors. Wiley-VCH, Weinheim, Germany. 453–472.

44. Sandhoff, K., E. Conzelmann, and H. Nehrkorn. 1977. Specificity of human liver hexosaminidases A and B against glycosphingolipids GM2 and GA2. Purification of the enzymes by affinity chromatography employing specific elution. *Hoppe Seylers Z. Physiol. Chem.* **358:** 779–787.

45. Conzelmann, E., K. Sandhoff, H. Nehrkorn, B. Geiger, and R. Arnon. 1978. Purification, biochemical and immunological characterisation of hexosaminidase A from variant AB of infantile GM2 gangliosidosis. *Eur. J. Biochem.* **84:** 27–33.

46. Sandhoff, K. 1970. The hydrolysis of Tay-Sachs ganglioside (TSG) by human N-acetyl-beta-D-hexosaminidase A. *FEBS Lett.* **11:** 342–344.

47. Li, S. C., and Y. T. Li. 1976. An activator stimulating the enzymic hydrolysis of sphingoglycolipids. *J. Biol. Chem.* **251:** 1159–1163.

48. te Vruchte, D., E. Lloyd-Evans, R. J. Veldman, D. C. Neville, R. A. Dwek, F. M. Platt, W. J. van Blitterswijk, and D. J. Sillence. 2004. Accumulation of glycosphingolipids in Niemann-Pick C disease disrupts endosomal transport. *J. Biol. Chem.* **279:** 26167–26175.

49. Pentchev, P. G., M. E. Comly, H. S. Kruth, M. T. Vanier, D. A. Wenger, S. Patel, and R. O. Brady. 1985. A defect in cholesterol esterification in Niemann-Pick disease (type C) patients. *Proc. Natl. Acad. Sci. USA.* **82:** 8247–8251.

50. Sasaki, H., H. Arai, M. J. Cocco, and S. H. White. 2009. pH dependence of sphingosine aggregation. *Biophys. J.* **96:** 2727–2733.

51. Schulze, H., and K. Sandhoff. 2014. Sphingolipids and lysosomal pathologies. *Biochim. Biophys. Acta.* **1841:** 799–810.

52. Suzuki, K. 1998. Twenty five years of the "psychosine hypothesis": a personal perspective of its history and present status. *Neurochem. Res.* **23:** 251–259.

53. Aerts, J. M., J. E. Groener, S. Kuiper, W. E. Donker-Koopman, A. Strijland, R. Ottenhoff, C. van Roomen, M. Mirzaian, F. A. Wijburg,

G. E. Linthorst, et al. 2008. Elevated globotriaosylsphingosine is a hallmark of Fabry disease. *Proc. Natl. Acad. Sci. USA.* **105:** 2812–2817.

54. Brügger, B., R. Sandhoff, S. Wegehingel, K. Gorgas, J. Malsam, J. B. Helms, W. D. Lehmann, W. Nickel, and F. T. Wieland. 2000. Evidence for segregation of sphingomyelin and cholesterol during formation of COPI-coated vesicles. *J. Cell Biol.* **151:** 507–518.

55. Mouritsen, O. G., and M. J. Zuckermann. 2004. What's so special about cholesterol? *Lipids.* **39:** 1101–1113.

56. Abe, A., and J. A. Shayman. 2009. The role of negatively charged lipids in lysosomal phospholipase A2 function. *J. Lipid Res.* **50:** 2027–2035.

57. Walkley, S. U., and M. T. Vanier. 2009. Secondary lipid accumulation in lysosomal disease. *Biochim. Biophys. Acta.* **1793:** 726–736.

58. Hepbildikler, S. T., R. Sandhoff, M. Kölzer, R. L. Proia, and K. Sandhoff. 2002. Physiological substrates for human lysosomal beta-hexosaminidase S. *J. Biol. Chem.* **277:** 2562–2572.

59. Harzer, K., and K. Sandhoff. 1971. Age-dependent variations of the human N-acetyl-β-D-hexosaminidases. *J. Neurochem.* **18:** 2041–2050.

60. Sandhoff, K. 1973. Multiple human hexosaminidases. *Birth Defects Orig. Artic. Ser.* **9:** 214–222.

61. Wendeler, M., J. Hoernschemeyer, D. Hoffmann, T. Kolter, G. Schwarzmann, and K. Sandhoff. 2004. Photoaffinity labelling of the human GM2-activator protein. Mechanistic insight into ganglioside GM2 degradation. *Eur. J. Biochem.* **271:** 614–627.

62. Conzelmann, E., and K. Sandhoff. 1978. AB variant of infantile GM2 gangliosidosis: deficiency of a factor necessary for stimulation of hexosaminidase A-catalyzed degradation of ganglioside GM2 and glycolipid GA2. *Proc. Natl. Acad. Sci. USA.* **75:** 3979–3983.

63. Mahuran, D. J. 1999. Biochemical consequences of mutations causing the GM2 gangliosidoses. *Biochim. Biophys. Acta.* **1455:** 105–138.

64. Bierfreund, U., T. Kolter, and K. Sandhoff. 2000. Sphingolipid hydrolases and activator proteins. *Methods Enzymol.* **311:** 255–276.

65. Kölzer, M., N. Werth, and K. Sandhoff. 2004. Interactions of acid sphingomyelinase and lipid bilayers in the presence of the tricyclic antidepressant desipramine. *FEBS Lett.* **559:** 96–98.

66. Locatelli-Hoops, S., N. Remmel, R. Klingenstein, B. Breiden, M. Rossocha, M. Schoeniger, C. Koenigs, W. Saenger, and K. Sandhoff. 2006. Saposin A mobilizes lipids from low cholesterol and high bis(monoacylglycero)phosphate-containing membranes: patient variant Saposin A lacks lipid extraction capacity. *J. Biol. Chem.* **281:** 32451–32460.

67. Hurwitz, R., K. Ferlinz, and K. Sandhoff. 1994. The tricyclic antidepressant desipramine causes proteolytic degradation of lysosomal sphingomyelinase in human fibroblasts. *Biol. Chem. Hoppe Seyler.* **375:** 447–450.

68. Sandhoff, K., and L. Quintern. 1988. Sphingolipid storage diseases of the central nervous system: bases of biochemical and clinical heterogeneity. *Naturwissenschaften.* **75:** 123–131.

69. Mansfield, P. J., S. S. Carey, V. Hinkovska-Galcheva, J. A. Shayman, and L. A. Boxer. 2004. Ceramide inhibition of phospholipase D and its relationship to RhoA and ARF1 translocation in GTP gamma S-stimulated polymorphonuclear leukocytes. *Blood.* **103:** 2363–2368.

70. Merrill, A. H., Jr., E. M. Schmelz, D. L. Dillehay, S. Spiegel, J. A. Shayman, J. J. Schroeder, R. T. Riley, K. A. Voss, and E. Wang. 1997. Sphingolipids—the enigmatic lipid class: biochemistry, physiology, and pathophysiology. *Toxicol. Appl. Pharmacol.* **142:** 208–225.

71. Goñi, F. M., and A. Alonso. 1999. Structure and functional properties of diacylglycerols in membranes. *Prog. Lipid Res.* **38:** 1–48.

72. Gómez-Fernández, J. C., and S. Corbalan-Garcia. 2007. Diacylglycerols, multivalent membrane modulators. *Chem. Phys. Lipids.* **148:** 1–25.

73. Contreras, F. X., A. V. Villar, A. Alonso, and F. M. Goni. 2009. Ceramide-induced transbilayer (flip-flop) lipid movement in membranes. *Methods Mol. Biol.* **462:** 155–165.

74. Montes, L. R., M. B. Ruiz-Arguello, F. M. Goni, and A. Alonso. 2002. Membrane restructuring via ceramide results in enhanced solute efflux. *J. Biol. Chem.* **277:** 11788–11794.

75. Zhang, Y., X. Li, K. A. Becker, and E. Gulbins. 2009. Ceramide-enriched membrane domains–structure and function. *Biochim. Biophys. Acta.* **1788:** 178–183.

76. Kolesnick, R. N. 1987. 1,2-Diacylglycerols but not phorbol esters stimulate sphingomyelin hydrolysis in GH3 pituitary cells. *J. Biol. Chem.* **262:** 16759–16762.

77. Fantini, J., and F. J. Barrantes. 2013. How cholesterol interacts with membrane proteins: an exploration of cholesterol-binding sites including CRAC, CARC, and tilted domains. *Front. Physiol.* **4:** 31.

78. Barnholz, Y., A. Roitman, and S. Gatt. 1966. Enzymatic hydrolysis of sphingolipids. II. Hydrolysis of sphingomyelin by an enzyme from rat brain. *J. Biol. Chem.* **241:** 3731–3737.

79. Quintern, L. E., E. H. Schuchman, O. Levran, M. Suchi, K. Ferlinz, H. Reinke, K. Sandhoff, and R. J. Desnick. 1989. Isolation of cDNA clones encoding human acid sphingomyelinase: occurrence of alternatively processed transcripts. *EMBO J.* **8:** 2469–2473.

80. Vance, D. E., and H. Van den Bosch. 2000. Cholesterol in the year 2000. *Biochim. Biophys. Acta.* **1529:** 1–8.

81. Tabas, I. 2002. Cholesterol in health and disease. *J. Clin. Invest.* **110:** 583–590.

82. Infante, R. E., M. L. Wang, A. Radhakrishnan, H. J. Kwon, M. S. Brown, and J. L. Goldstein. 2008. NPC2 facilitates bidirectional transfer of cholesterol between NPC1 and lipid bilayers, a step in cholesterol egress from lysosomes. *Proc. Natl. Acad. Sci. USA.* **105:** 15287–15292.

83. Friedland, N., H. L. Liou, P. Lobel, and A. M. Stock. 2003. Structure of a cholesterol-binding protein deficient in Niemann-Pick type C2 disease. *Proc. Natl. Acad. Sci. USA.* **100:** 2512–2517.

84. Vanier, M. T. 2015. Complex lipid trafficking in Niemann-Pick disease type C. *J. Inherit. Metab. Dis.* **38:** 187–199.

85. Nilsson, O., and L. Svennerholm. 1982. Accumulation of glucosylceramide and glucosylsphingosine (psychosine) in cerebrum and cerebellum in infantile and juvenile Gaucher disease. *J. Neurochem.* **39:** 709–718.

86. Vanier, M., and L. Svennerholm. 1976. Chemical pathology of Krabbe disease: the occurrence of psychosine and other neutral sphingoglycolipids. *Adv. Exp. Med. Biol.* **68:** 115–126.

87. Rodriguez-Lafrasse, C., and M. T. Vanier. 1999. Sphingosylphosphorylcholine in Niemann-Pick disease brain: accumulation in type A but not in type B. *Neurochem. Res.* **24:** 199–205.

88. Sarmientos, F., G. Schwarzmann, and K. Sandhoff. 1986. Specificity of human glucosylceramide beta-glucosidase towards synthetic glucosylsphingolipids inserted into liposomes. Kinetic studies in a detergent-free assay system. *Eur. J. Biochem.* **160:** 527–535.

89. Lloyd-Evans, E., A. J. Morgan, X. He, D. A. Smith, E. Elliot-Smith, D. J. Sillence, G. C. Churchill, E. H. Schuchman, A. Galione, and F. M. Platt. 2008. Niemann-Pick disease type C1 is a sphingosine storage disease that causes deregulation of lysosomal calcium. *Nat. Med.* **14:** 1247–1255.

90. Anheuser, S., B. Breiden, and K. Sandhoff. 2019. Ganglioside GM2 catabolism is inhibited by storage compounds of mucopolysaccharidoses and by cationic amphiphilic drugs. *Mol. Genet. Metab.* In press.

91. Leinekugel, P., S. Michel, E. Conzelmann, and K. Sandhoff. 1992. Quantitative correlation between the residual activity of beta-hexosaminidase A and arylsulfatase A and the severity of the resulting lysosomal storage disease. *Hum. Genet.* **88:** 513–523.

92. Sandhoff, K., and K. Harzer. 2013. Gangliosides and gangliosidoses: principles of molecular and metabolic pathogenesis. *J. Neurosci.* **33:** 10195–10208.

93. Giehl, A., T. Lemm, O. Bartelsen, K. Sandhoff, and A. Blume. 1999. Interaction of the GM2-activator protein with phospholipid-ganglioside bilayer membranes and with monolayers at the air-water interface. *Eur. J. Biochem.* **261:** 650–658.

94. Linke, T. 2000. Purification, Enzymatic Characterization and Interfacial Activity of Human Acid Ceramidase—the Role of Sphingolipid Activator Proteins in Ceramide Degradation. PhD Thesis: University of Bonn, Bonn, Germany.

95. Vogel, A., G. Schwarzmann, and K. Sandhoff. 1991. Glycosphingolipid specificity of the human sulfatide activator protein. *Eur. J. Biochem.* **200:** 591–597.

96. Lüllmann, H., R. Lüllmann-Rauch, and O. Wassermann. 1973. Drug-induced phospholipidosis. *Ger. Med.* **3:** 128–135.

97. Lüllmann, H., R. Lüllmann-Rauch, and O. Wassermann. 1978. Lipidosis induced by amphiphilic cationic drugs. *Biochem. Pharmacol.* **27:** 1103–1108.

98. Möbius, W., V. Herzog, K. Sandhoff, and G. Schwarzmann. 1999. Gangliosides are transported from the plasma membrane to intralysosomal membranes as revealed by immuno-electron microscopy. *Biosci. Rep.* **19:** 307–316.

99. Möbius, W., V. Herzog, K. Sandhoff, and G. Schwarzmann. 1999. Intracellular distribution of a biotin-labeled ganglioside, GM1, by immunoelectron microscopy after endocytosis in fibroblasts. *J. Histochem. Cytochem.* **47:** 1005–1014.

100. Klumperman, J., and G. Raposo. 2014. The complex ultrastructure of the endolysosomal system. *Cold Spring Harb. Perspect. Biol.* **6:** a016857.

101. Vanier, M. T. 1999. Lipid changes in Niemann-Pick disease type C brain: personal experience and review of the literature. *Neurochem. Res.* **24:** 481–489.

102. Vance, J. E. 2006. Lipid imbalance in the neurological disorder, Niemann-Pick C disease. *FEBS Lett.* **580:** 5518–5524.